

A Signal-to-Noise Model for ELF Propagation in Subsurface Regions

Colin P. Burke and D. Llanwyn Jones

Abstract— Measurements of the natural extremely low-frequency (ELF) radio noise (known as Schumann resonances) in the period 1988–1989 have enabled average atmospheric noise levels and Schumann resonance parameters to be deduced. At 45 Hz, the average measured electric field was $41.6 \text{ dB} \cdot \mu\text{V}/\text{m} \cdot \sqrt{\text{Hz}}$. It is assumed that the Schumann resonance noise field in the air-space in the vicinity of the observation point can be considered to be represented as the sum of four components, one arising from propagation over a short great-circle path, and a second representing a long great-circle path contribution, each of these having an upgoing and a downgoing part. The noise fields can then be estimated at any given depth below the ground (or sea) surface from the measured values in the air. We present results showing the computed fields produced in the sea from submerged horizontal electric quadrupole and vertical electric dipole man-made sources, and compare these with the subsurface atmospheric noise fields deduced from the experimental measurements.

I. INTRODUCTION

THE natural ELF (3 Hz–3 kHz) radio noise in the Earth-ionosphere duct caused by global lightning activity (known as Schumann resonances in the lower part of the ELF band) consists of an essentially vertical electric field and a horizontal magnetic field. The Schumann resonances are simply the atmospheric noise fields produced in the Earth-ionosphere spherical shell cavity resonator by global lightning activity. The attenuation of electromagnetic waves propagating over the Earth's surface is small in the lower part of the ELF band (about 0.2 dB/Mm at 5 Hz) and increases with a frequency increase. This has the consequence that lightning-produced radio noise is of a quasi-continuous nature in the lower ELF band, but becomes impulsive in the upper part of the band where the attenuation exceeds 30 dB/Mm. The atmospheric noise field penetrates the ground or sea surface, and thus produces a limit to the fields produced by a buried or underwater source that can be detected successfully.

In this work, we are concerned with the development of a signal-to-noise model applied to the case of subsurface vertical and horizontal electric and magnetic dipoles (VED, HED, VMD, and HMD) and horizontal electric quadrupoles (HEQ). Many workers have been concerned with the problem of calculating the radiation from buried or submerged sources, but the interest is usually in computing the fields in air.

Manuscript received August 16, 1993. This work was supported by the U.K. Science and Engineering Research Council under Grant SGD 10351 and by the Defence Research Agency, Portland, U.K.

The authors are with the Department of Physics, King's College, London WC2R 2LS, England.

IEEE Log Number 9403034.

Our interest is in the subsurface fields. The ELF band is particularly relevant in this context because of the relatively low attenuation (or large skin depth) experienced by the waves in conducting media such as sea water.

In general, electromagnetic fields may be calculated from Hertz vectors defined in terms of the Sommerfeld integrals. Usually, these integrals cannot be evaluated analytically, and the fields are thus normally computed numerically. Weaver [1] presents formulas to calculate the fields due to vertical electric and horizontal dipoles in a three-layer medium. Fraser-Smith *et al.* [2] considered dipole sources located on the sea floor radiating in an infinitely deep sea. In a series of papers (for example, [3], [4]), Bannister presents a series of simple, algebraic formulas to evaluate the fields due to dipoles in two-layer media subject to certain restrictions on the refractive index of the interface between the two semi-infinite layers. Lindell and Alanen [5]–[7] have produced an exact image theory (EIT) for dipoles radiating in a two-layer medium, and the resulting integral expressions are more rapidly convergent than the original Sommerfeld integrals.

Warber and Field have produced a long-wave noise prediction model [8] which predicts atmospheric noise on a global basis in the frequency ranges 50–300 Hz and 10–60 kHz. The model allows for the occurrence rate of lightning flashes as a function of time of day, season, and geographic position. The propagation component of the model makes allowances for the variations of ionospheric parameters and ground conductivity along the propagation path. To date, however, it appears that there are few publications in which the signal-to-noise problem for subsurface communication has been tackled in the Schumann resonance part of the ELF band, i.e., in the range 5–50 Hz.

Since the first convincing experimental confirmation by Balsler and Wagner [9] of Schumann's seminal theoretical work [10], many workers have observed the resonance phenomenon: Rycroft [11] observed the diurnal changes in the resonance frequencies, as did Chapman and Jones [12] who compared the measured frequencies and Q factors of the resonances with the predictions given by a two-layer model of the ionosphere. Ogawa *et al.* [13] observed Schumann resonances with a balloon in the stratosphere, and the first seven modes could be distinguished. Sentman [14] presents an analysis of the polarization of ELF radiation and references recent experimental work.

From our experimental measurements of Schumann resonances, we have been able to estimate the average electromagnetic noise in the Earth-ionosphere cavity in the band 5–45

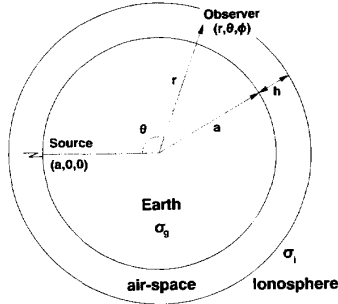


Fig. 1. The Earth-ionosphere geometry.

Hz at a recording station located in southern England. These measurements enable atmospheric noise levels in the sea or subsurface strata to be computed. We have also evaluated the Sommerfeld integrals numerically for the VED, HED, VMD, HMD, and HEQ subsurface sources. Here, we illustrate the results of such work for HEQ and VED radiators.

II. SCHUMANN RESONANCES

Following from the work of Schumann [10], Wait [15], and Galejs [16], in geocentric spherical polar coordinates (r, θ, ϕ) , the Earth is considered to be a perfectly conducting sphere of radius a surrounded by a laterally homogeneous ionosphere of conductivity σ_i , permittivity ϵ_i , and radius $r = a + h$ (see Fig. 1). The fields at an angular distance θ from the source produced by a VED (which is used to represent a lightning flash) located at $(a, 0, 0)$ are given to good accuracy by

$$E_r = \frac{iIds\nu(\nu+1)}{4a^2\epsilon_0\omega h} \frac{P_\nu(-\cos\theta)}{\sin\pi\nu} \\ = -\frac{iIds\nu(\nu+1)}{4\pi a^2\epsilon_0\omega h} \sum_{n=0}^{\infty} \frac{(2n+1)}{n(n+1)-\nu(\nu+1)} P_n(\cos\theta) \quad (1)$$

$$H_\phi = \frac{-Ids P_\nu^1(-\cos\theta)}{4ah} \frac{1}{\sin\pi\nu} \\ = -\frac{Ids}{4\pi ah} \sum_{n=0}^{\infty} \frac{(2n+1)}{n(n+1)-\nu(\nu+1)} P_n^1(\cos\theta) \quad (2)$$

where

$$\nu(\nu+1) = k^2 a^2 S^2. \quad (3)$$

ν is the modal eigenvalue which, in general has to be determined numerically as the root of a transcendental equation. In the equations above, Ids is the current moment of the source VED, $i = \sqrt{-1}$, $P_\nu^{0,1}(-\cos\theta)$ are Legendre functions of (complex) degree ν and order 0, 1, $P_n^{0,1}(\cos\theta)$ are the zonal harmonic functions of degree n and order 0, 1, ω is the angular frequency, $k = \omega/c$, and S is the sine of the complex angle of incidence of the fields on the ionosphere. These equations are also applicable to the real situation in which the ionospheric boundary is diffuse, but the computation of ν is then more involved [16], [17].

For a given value of $n = 0, 1, 2, \dots$, the fields take their maximum values near where $|n(n+1) - \nu(\nu+1)|$ is a minimum. Thus, the resonances occur approximately at frequencies given by

$$f_n = \frac{c}{2\pi a} \frac{\sqrt{n(n+1)}}{Re S}. \quad (4)$$

$Re S$ is about 1.3 in the Schumann resonance band [17], and the measured resonant frequencies for the first three modes occur at about 7.8, 14, and 19 Hz.

A. Atmospheric Noise Spectra

Following Galejs [16], the electric-field power spectrum due to a distribution of VED's (lightning strokes) is given by

$$G^E(i\omega) = \int_0^{2\pi} \int_0^\pi g(i\omega, \theta, \phi) a^2 \sin\theta \\ \cdot \left| \frac{\nu(\nu+1) P_\nu(-\cos\theta)}{4\epsilon_0 a^2 \omega h \sin\pi\nu} \right|^2 d\theta d\phi \quad (5)$$

where $g(i\omega, \theta, \phi)$ is proportional to the squared moment of the source per unit area of the globe's surface, and it is assumed that [16]

$$g(i\omega, \theta, \phi) = g(i\omega) \sim \text{const} \times \exp(-0.0091\omega) \quad (6)$$

for $\theta_1 < \theta < \theta_2$ and is zero elsewhere, i.e., the sources are distributed within a range of distances from the observer and do not exhibit a systematic geographical variation in their characteristics. Thus, (5) becomes

$$G^E(i\omega) = \text{const}' \times \int_{\theta_1}^{\theta_2} g(i\omega) a^2 \sin\theta \\ \cdot \left| \frac{\nu(\nu+1) P_\nu(-\cos\theta)}{4\epsilon_0 a^2 \omega h \sin\pi\nu} \right|^2 d\theta. \quad (7)$$

If $\nu = \nu(\omega)$ is known, then θ_1 , θ_2 , and the constant can be estimated by using an optimization (or curve-fitting) algorithm to minimize the function

$$R = \sum \left(\sqrt{G^E(\omega, \theta)} - \sqrt{G_M^E(\omega, \theta)} \right)^2 \quad (8)$$

where G_M^E is the average of experimentally measured electric Schumann spectra and G^E is the theoretical value computed from (7). The square root of the power spectra has been used because these are less "spiky" in nature than the power spectra themselves.

When the values of θ_1 and θ_2 have been estimated from the curve-fitting process, the average theoretical magnetic Schumann power spectrum $G^H(i\omega)$ can then be calculated from

$$G^H(i\omega) = \text{const}' \times \int_{\theta_1}^{\theta_2} g(i\omega) a^2 \sin\theta \\ \cdot \left| \frac{Ids P_\nu^1(-\cos\theta)}{4ah \sin\pi\nu} \right|^2 d\theta. \quad (9)$$

It is computationally advantageous to use the Legendre function $P_\nu^{0,1}(-\cos\theta)$ representations for the fields rather than

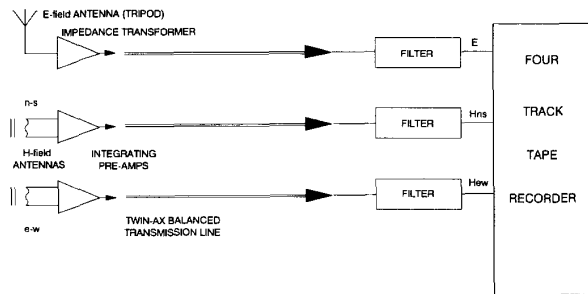


Fig. 2. Schematic of the ELF receiving equipment.

employing the zonal harmonics $P_n^{0,1}(\cos \theta)$ of (1) and (2). Suitable algorithms for calculating these functions by means of a microcomputer have been described by Jones and Joyce [18] and Jones and Burke [19].

It should be pointed out that this process does not serve to locate the real active thunderstorm centers because at any one time, there are likely to be at least two such large-scale zones centered on specific values of θ and ϕ . However, the curve fit *does* provide an average "theoretical" Schumann spectrum, and enables the magnetic spectrum of atmospheric noise to be computed from measured electric field data.

B. Experimental Observations

A system for recording ELF bursts in the 5–45 Hz band is described by Burke and Jones [20]. The system was used to determine the latitude dependence of the attenuation constant in the 5–45 Hz band, and the measurements taken have provided information on the variation of ν with frequency. The system was also capable of recording Schumann resonances, and this was carried out on selected days in the period June 1988–August 1989 at two sites in southern England.

A block diagram of the apparatus is given in Fig. 2. A variant upon a whip antenna in the form of a tripod was used to detect the vertical electric field. Vibration of the antenna in the Earth's natural electrostatic field produced by the wind and movement of naturally occurring space charges produces large, unwanted signals at the lower frequencies. Some degree of this contaminating noise was always present despite the presence of high-pass filters to ameliorate its effects. Because the magnetic field vector lies essentially in the horizontal plane, two antennas, one oriented north–south, the other east–west, serve to define the field. Both the electric and magnetic systems incorporated power-line-frequency and associated harmonics rejection filters.

Great care was taken to calibrate the electric and magnetic field systems accurately. The calibration of the magnetic systems was effected in two stages. A secondary (local) calibration used small coils wound on to the main aerial bobbins. By injecting pulses into these coils and comparing the output of the receiving system with the input signal in the frequency domain using a low-frequency spectrum analyzer (Hewlett Packard, Model 3582A), the frequency response of both magnetic systems could be determined. The absolute

sensitivities of each magnetic antenna were measured by a "remote" calibration procedure. This consisted of creating a known magnetic field in the vicinity of each antenna and noting the output response. The known field was produced by the amplified signal from a sine wave oscillator driving a remote calibration coil located some tens of meters from the receiving solenoid. The correction to the computed field for the ground effect was completely negligible as the remote calibration source was located at distances which were very small compared to the skin depth in the ground [21]. A sine wave was chosen for the remote calibration rather than the broad-band signals used for the secondary calibration because the broad-band signals gave a poor signal-to-noise ratio in this case. The midband absolute sensitivity of the magnetic field systems was about 3 V/nT (measured at the input of the tape recorder).

For the electric-field system, it was not possible to create a uniform electric field about the antenna owing to its size, so a different approach was adopted. First, the frequency response of the electronic system was established by using the spectrum analyzer. For this calibration, the antenna was disconnected, and the system was driven by a signal generator via a 75 pF capacitor dummy antenna to represent the known aerial capacitance. The effective height of the antenna was then determined using transmissions from the 16 kHz Rugby VLF (GBR) station. This was done by comparing the signal voltage received by the electric-field antenna with that obtained using an accurately constructed parallel plate antenna whose effective height was well defined. In this way, the effective height of the tripod antenna was estimated as 1.01 ± 0.03 m, and the overall absolute sensitivity of the system was about 7 m (i.e., 7 V/V/m), again measured at the input of the tape recorder.

The atmospheric noise data were recorded on the tape recorder, and later played back through the spectrum analyzer. Each spectrum was recorded over an approximately 10 min interval, the maximum duration that could be set on the analyzer.

The recorded magnetic spectra were generally more contaminated by narrow-band noise of local origin than were the electric, except at the lowest frequencies, so the better quality electric spectra have been used in the curve-fitting process.

Fig. 3 shows an example of a single electric Schumann spectrum. Resonances can be clearly observed at about 14, 19, and 26 Hz; however, the first-order resonance is obscured by the low-frequency noise referred to above. The average of some 27 such spectra is illustrated in Fig. 4. Again, the first-order mode at about 8 Hz is obscured by low-frequency noise. Evidence of resonances at about 14, 19, 26, and 32 Hz can be seen. There are some indications of a mode at 38 Hz corresponding to the sixth-order resonance. The large spike at 50 Hz is due to power-line-frequency transmissions. The resonance peaks and valleys are still "spiky" despite the averaging process, and this reflects the very spiky nature of the original spectra. This is compounded by the fact that not all of the whole 27 spectra could be averaged for every resonance mode. Particular problems were experienced with the second mode (14 Hz) where a local interference source operating at a center frequency of 16 Hz often contaminated the resonance.

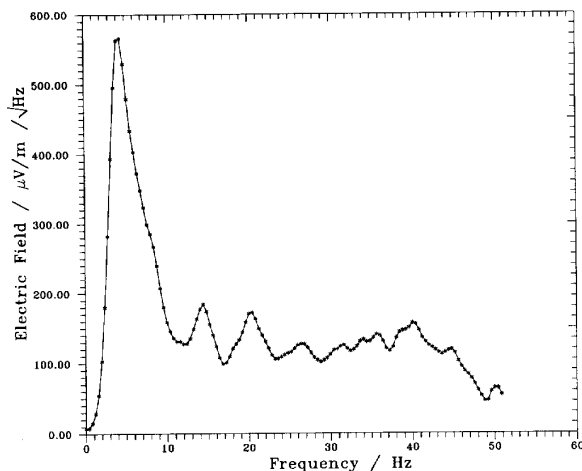


Fig. 3. A typical electric-field Schumann resonance spectrum.

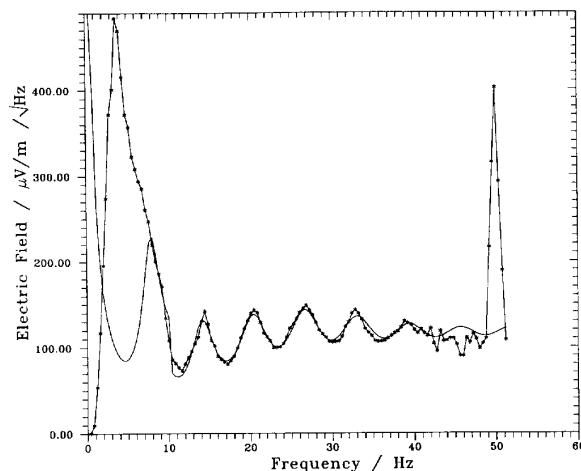


Fig. 5. The theoretical fit to the average electric-field Schumann spectrum.

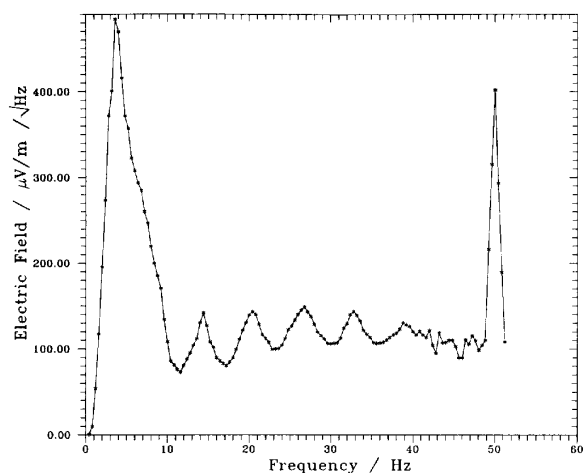


Fig. 4. The average electric-field Schumann spectrum.

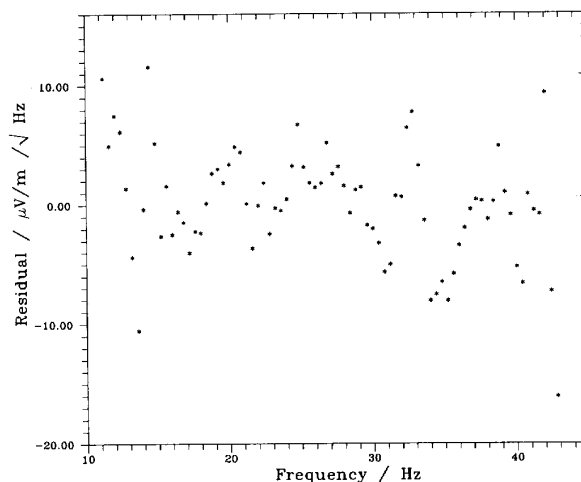


Fig. 6. The residuals from the curve fit as a function of frequency.

The average measured rms electric field at 45 Hz is $41.6 \text{ dB} \cdot \mu\text{V/m} \cdot \sqrt{\text{Hz}}$. The long-wave noise prediction model (LNP) program [8], run for the geographical location of our measurements at 50 Hz (the lowest frequency for which the model is designed), predicts field strengths of $49.88 \pm 13.16 \text{ dB} \cdot \mu\text{V/m} \cdot \sqrt{\text{Hz}}$ at 12 UT for January and $52.39 \pm 12.88 \text{ dB} \cdot \mu\text{V/m} \cdot \sqrt{\text{Hz}}$ at 12 UT for July. From the above, it appears that the lower estimates of the LNP most closely match our measured electric-field noise values.

In Fig. 5, a theoretical fit to the average spectrum has been carried out using the methods described above. The curve fit was made in the range 11–43 Hz. In general, the fit is good, except at the higher frequencies where the measured data become noisy. This is reflected in the behavior of the residuals $r = \sqrt{G_M^E(\omega_i)} - \sqrt{G^E(\omega_i)}$, i.e., the difference between the observed and fitted spectra. These residuals are plotted as a function of frequency in Fig. 6, and it can be seen that increasing amounts of scatter occur at higher frequency.

C. Effect of Natural Noise on Subsurface Communication Systems

Our principal interest is the computation of noise fields in a sea of depth d . However, the formation applies equally to other three-layer stratified media. In the immediate vicinity of the observer, the Schumann resonance noise field in the air-space produced by distant sources can be regarded as arising from four propagating plane waves. Two wave fields arise from short-path and long-path propagation around the globe. One of these corresponds to a wave that has traveled from the thunderstorm center to the observation point via the short great-circle path, and the other has traveled on the long great-circle path (being the "around-the-world" signal). These two wave systems are needed to represent the Schumann resonance effect. For each of these, there is a downgoing wave (produced by ionospheric reflections) which is incident upon the surface of the ground (or sea) at a complex angle (the waveguide-mode eigenangle) whose sine is λ/k_1 , and an upgoing wave

(produced by ground reflection). Note that the symbol “ λ ” here is Sommerfeld’s variable and not the wavelength.

The local fields are defined in a Cartesian coordinate system (x, y, z) in which $z = 0$ is the sea surface, z is directed downwards, and $x = a\theta$ with θ being as defined previously—see Fig. 7. In this system, we assume that the magnetic field in the air only has a y component. The total magnetic field corresponding to that which would be measured at the Earth’s surface is then represented as the sum of the short-path and the long-path contributions as follows:

$$H_{y1}^T = H_{y1} + H_{y1}' \quad (10)$$

with

$$H_{y1} = a_1 e^{-i\lambda x} e^{-u_1 z} (1 + r e^{2u_1 z}) \quad (11)$$

$$H_{y1}' = a_1' e^{i\lambda x} e^{-u_1 z} (1 + r e^{2u_1 z}) \quad (12)$$

where a_1 and a_1' are the (unknown) incident field amplitudes and r is the effective reflection coefficient of the ground, which includes a contribution arising from the lower interface.

It can be shown that the *total* electric and magnetic atmospheric noise fields (\mathbf{E}, \mathbf{H}) in the sea can be expressed in terms of the measured noise field in the air-space H_{y1}^T by

$$H_{y2} = [A e^{-u_2 x} + B e^{u_2 z}] H_{y1}^T \quad (13)$$

and

$$E_{x2} = (u_2 / \sigma_2^*) [A e^{-u_2 z} - B e^{u_2 z}] H_{y1}^T, \quad E_{z2} \ll E_{x2}. \quad (14)$$

The coefficients A and B in (13) and (14) are found straightforwardly by application of the usual boundary conditions at the air–sea ($z = 0$) and the sea–seabed ($z = d$) interfaces. The result is

$$A = \frac{1}{1 + R_{23}^{\parallel} e^{-2u_2 d}} \quad (15)$$

$$B = A R_{23}^{\parallel} e^{-2u_2 d}. \quad (16)$$

In (11)–(16),

$$\lambda = k_1 S \quad (17)$$

$$\sigma_j^* = \sigma_j + i\epsilon_j \omega, \quad j = 1, 2, 3 \quad (18)$$

$$u_j = \sqrt{\lambda^2 - k_j^2} \quad (19)$$

$$R_{23}^{\parallel} = \frac{u_2 \sigma_3^* - u_3 \sigma_2^*}{\sigma_2^* u_3 + \sigma_3^* u_2}. \quad (20)$$

For the air-space $j = 1$, $j = 2, 3$ for the sea and seabed, respectively, and R_{23}^{\parallel} is the reflection coefficient of the lower interface for vertically polarized waves. Values of S as a function of frequency are obtained from (3) using the known variation of the of the model eigenvalue ν with frequency [20]. Note that it is not necessary to know the two incident field amplitudes a_1 and a_1' to compute the total field in the sea.

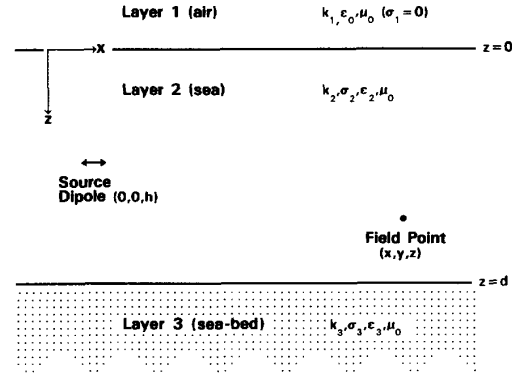


Fig. 7. The air–sea–seabed geometry.

III. THE FIELDS PRODUCED IN THE SEA DUE TO SUBMERGED SOURCES

The fields produced by submerged VED and HED sources have been described by Burke and Jones [22]. The fields due to the corresponding VMD and HMD can be obtained from those of the electric dipoles by making the substitutions described in the Appendix. Here, we are also interested in horizontal electric quadrupole (HEQ) sources. The quadrupole moment of an electric quadrupole is a second rank tensor; six different configurations exist with the quadrupole moments designated M_{ij}^Q with $ij = xx, xy, xz, yy, yz, \text{ or } zz$. We consider the “ xx ” HEQ which consists of two HED’s of current moment $I ds$ located “end to end,” one in the $+x$ direction and the other in the $-x$ direction. If the separation of the dipoles is Δx and if V is any potential or field component at the point (x, y, z) , then

$$V^Q = -\Delta x \frac{\partial V^D}{\partial x} \quad (21)$$

where superscripts D and Q are attached to dipole and quadrupole quantities, respectively. The fields of the HEQ can thus be obtained from the previously reported formulas for the HED [22]. The resulting expressions involve integrals of the Sommerfeld type.

These Sommerfeld integrals for the HEQ have been evaluated numerically using a variant on Gaussian quadrature and the Shanks–Wynn algorithm to speed up convergence. As an example of the calculations made, Fig. 8 shows the modulus of the total field B due to a time-harmonic HEQ as a function of frequency in the range 8–45 Hz. The dipole has a moment $M_{xx}^Q = I ds \Delta x = 0.3 \text{ A}\cdot\text{m}^2$, and is located at a depth of 5 m, in a sea of conductivity 4 S/m, 20 m deep, with a seabed conductivity of 0.6 S/m.

The fields have been calculated at the points (30, 30, 6), (35, 35, 6), (40, 40, 6), and (50, 50, 6). The broken curve shows the estimated natural Schumann noise at that depth [computed from the data of Fig. 5 and (13)] assuming the receiver to have a 1 Hz bandwidth. The effects of the noise on the communication system depends, of course, on the noise bandwidth of the receiver, but can readily be computed from the data presented for various receiver bandwidths.

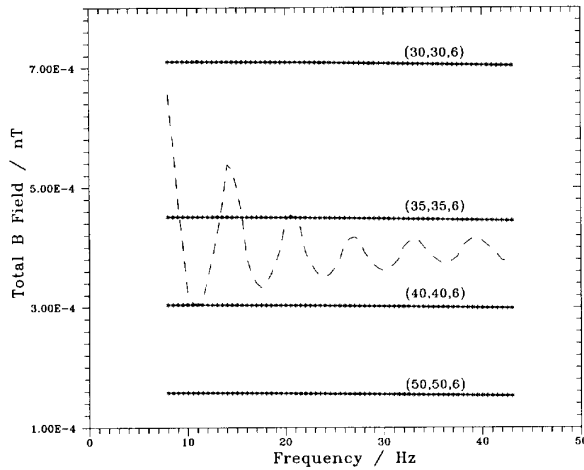


Fig. 8. Total B field due to HEQ source and estimated Schumann noise.

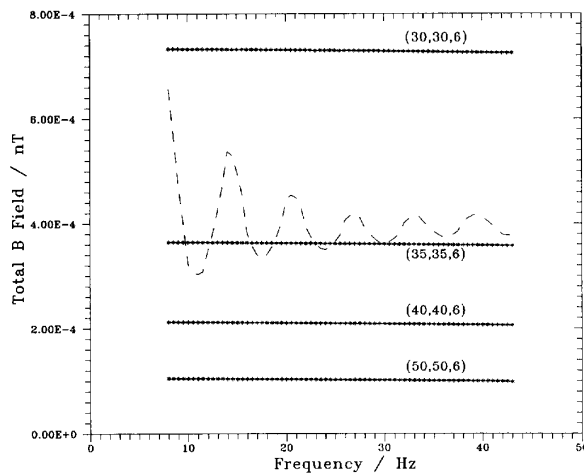


Fig. 9. Total B field due to VED source and estimated Schumann noise.

For comparison, Fig. 9 shows the corresponding data for a VED source with a current moment of 0.3 A·m at the same values of the range. An obvious feature of the fields produced by both sources is that for a given source–observer separation (or range), the field values stay approximately constant as the frequency increases. At first sight, this may seem contrary to that which is expected. Considering a dipole in an infinite medium, as the frequency increases, the skin depth decreases so, at a given distance from the source, the fields at the higher frequencies are expected to decrease. At 50 Hz, the skin depth in seawater is 36 m, so this effect could be expected to be evident in the data presented here. However, in electrically shallow seas, the effect of the two interfaces is to give rise to two lateral waves guided by the interfaces. The infinite-medium field is then termed the primary field and the lateral waves the secondary field. It is this secondary field, increasing with a frequency increase, which, in the examples above, counteracts the effect of the decreasing primary field so that the total field is very nearly constant over this frequency band.

IV. CONCLUSIONS

Measurements of the natural electromagnetic noise field in the lower ELF band called Schumann resonances have enabled estimates to be made of the natural noise at any depth in seawater. This, combined with the numerical evaluation of Sommerfeld integrals, has enabled a signal-to-noise model for ELF propagation in seawater for VED, HED, VMD, HMD, and HEQ sources to be produced.

APPENDIX

It follows from the symmetry in Maxwell's equations that the field expressions for magnetic dipole sources can be obtained from those obtained previously for the electric sources (Burke and Jones [22]). This is achieved by making the following substitutions in the VED and HED field equations:

$$\sigma^* \rightarrow i\omega\mu$$

$$i\omega\mu \rightarrow \sigma^*$$

$$E \rightarrow H$$

$$H \rightarrow -E$$

$$R_{mn} \rightarrow R_{mn}^{\parallel}$$

$$R_{mn}^{\parallel} \rightarrow R_{mn}$$

and

$$\frac{Ids}{4\pi\sigma^*} \rightarrow \frac{Ida}{4\pi}$$

where Ids is the current moment of the electric dipole, Ida is that of the magnetic dipole, and R_{mn} and R_{mn}^{\parallel} are the reflection coefficients of the interfaces for horizontal and vertical polarizations, respectively.

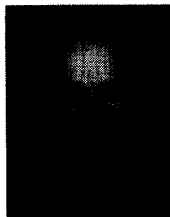
ACKNOWLEDGMENT

We express our thanks to C. R. Warber, Pacific-Sierra Research Corporation, for giving us access to the long-wave noise prediction computer program.

REFERENCES

- [1] J. T. Weaver, "The quasi-static field of an electric dipole embedded in a two layer conducting half space," *Can. J. Phys.*, vol. 45, pp. 1981–2002, 1967.
- [2] A. C. Fraser-Smith, A. S. Inan, O. G. Villard, Jr., and R. G. Joiner, "Seabed propagation of ULF/ELF electromagnetic fields from harmonic dipole sources," *Radio Sci.*, vol. 23, pp. 931–944, 1988.
- [3] P. R. Bannister, "New simplified formulas for ELF subsurface-to-subsurface propagation," *IEEE J. Oceanic Eng.*, vol. OE-9, pp. 154–163, 1984.
- [4] ———, "Applications of complex image theory," *Radio Sci.*, vol. 21, pp. 605–616, 1986.
- [5] I. V. Lindell and E. Alanen, "Exact image theory for the Sommerfeld half-space problem, Part I: Vertical magnetic dipole," *IEEE Trans. Antennas Propagat.*, vol. AP-32, pp. 126–133, 1984.
- [6] ———, "Exact image theory for the Sommerfeld half-space problem, Part II: Vertical electric dipole," *IEEE Trans. Antennas Propagat.*, vol. AP-32, pp. 841–847, 1984.

- [7] ———, "Exact image theory for the Sommerfeld half-space problem, Part III: General formulation," *IEEE Trans. Antennas Propagat.*, vol. AP-32, pp. 1027–1032, 1984.
- [8] C. R. Warber and E. C. Field, Jr., *Long Wave Noise Prediction, Vols. 1, 2 and 3*, Pacific-Sierra Res. Corp., 12340 Santa Monica Blvd., Los Angeles, CA 90025 (Contract DNA-001-87-C-0171: vol. 1, 2, and 3), 1991.
- [9] M. Balsler and C. A. Wagner, "Observations of earth-ionosphere cavity resonances," *Nature*, vol. 188, pp. 638–641, 1960.
- [10] W. O. Schumann, "Electrical selfoscillations of the earth-air-ionosphere cavity," (in German), *Z. Angew. Phys.*, vol. 9, pp. 373–378, 1957.
- [11] M. J. Rycroft, "Resonances of the earth-ionosphere cavity observed at Cambridge, England," *Radio Sci.*, vol. 69D, no. 8, pp. 1071–1081, 1965.
- [12] F. W. Chapman and D. L. Jones, "Observations of earth-ionosphere cavity resonances and their interpretation in terms of a two-layer ionosphere model," *Radio Sci., J. Res. NBS*, vol. 68D, no. 11, pp. 1177–1185, 1964.
- [13] T. Ogawa and H. Kozai Kawamoto, "Schumann resonances observed in a balloon in the stratosphere," *J. Atmos. Terr. Phys.*, vol. 41, pp. 135–142, 1979.
- [14] D. D. Sentman, "Approximate Schumann resonance parameters for a two-scale-height ionosphere," *J. Atmos. Terr. Phys.*, vol. 52, pp. 35–46, 1990.
- [15] J. R. Wait, *Electromagnetic Waves in Stratified Media*, 2nd ed. Oxford: Pergamon, 1972, ch. 6.
- [16] J. Galejs, *Terrestrial Propagation of Long Electromagnetic Waves*. Oxford: Pergamon, 1972, ch. 4, 7.
- [17] D. L. Jones, "Schumann resonances and ELF propagation for inhomogeneous, isotropic ionosphere models," *J. Atmos. Terr. Phys.*, vol. 29, pp. 1037–1044, 1967.
- [18] D. L. Jones and G. S. Joyce, "The computation of ELF radio wave fields in the earth-ionosphere duct," *J. Atmos. Terr. Phys.*, vol. 51, pp. 233–239, 1989.
- [19] D. L. Jones and C. P. Burke, "Zonal harmonic series expansion of Legendre functions and associated Legendre functions," *J. Phys. A: Math. Gen.*, vol. 23, pp. 3159–3168, 1990.
- [20] C. P. Burke and D. L. Jones, "An experimental investigation of ELF attenuation rates in the earth-ionosphere duct," *J. Atmos. Terr. Phys.*, vol. 54, pp. 243–250, 1992.
- [21] J. R. Wait, *Geo-Electromagnetism*. New York: Academic, 1982, ch. 3.
- [22] C. P. Burke and D. L. Jones, "ELF propagation in deep and shallow sea water," in *Proc. 51st Symp. Electromagn. Wave Propagation Panel of AGARD (NATO)*, Brussels, Belgium, Sept. 1992, pp. 11/1–11/7 (to be published by AGARD, 7 Rue Ancelle 9200, Neuilly sur Seine, France).



Colin P. Burke was born in Rochester, England, on October 19, 1962. He received the B.Sc. degree in 1987 and the Ph.D. degree in 1992, both from King's College.

From 1981 to 1984 he worked in the international nonmarine insurance market at Lloyd's of London, and then worked for a financial consultancy. His research has been in the areas of ELF propagation in the Earth-ionosphere duct and radio wave propagation in layered media.



D. Llanwyn Jones was born in Sutton Coldfield, England, on February 14, 1938. He received the B.Sc. and Ph.D. degrees from the University of London, King's College, in 1960 and 1963, respectively.

At King's College, he was appointed to a Lectureship in 1962 and to a Readership, his current post, in 1972. He has led the Radiophysics Group since 1972. He has held Visiting Professorships at the University of Colorado in 1968–1969, the University of Nagoya (Japan) in 1975, and the University of Kochi (Japan) in 1987. In Colorado,

he was one of the first Visiting Fellows of the Cooperative Institute for Research in Environmental Sciences. His research work has been in the theory and observation of the propagation of ELF and VLF radio waves in the Earth-ionosphere duct and in the radio emissions from lightning. His enduring interest has been in experimental and theoretical aspects of the Schumann resonances. More recently, his research has developed in the theory and computation of ionospheric and subsurface radio waves.